Robust construction of the extended three-dimensional flow complex

Frédéric Cazals

INSTITUT NATIONAL DE RECHERCHE EN INFORMATIQUE ET EN AUTOMATIQUE

Robust construction of the extended three-dimensional flow complex

Frédéric Cazals

N° 5903

Avril 2006

Thème SYM

ISSN 0249-6399

Robust construction of the extended three-dimensional flow complex

Frédéric Cazals

Thème SYM — Systèmes symboliques
Projet Geometrica

Rapport de recherche n° 5903 — Avril 2006 — 23 pages

Abstract: The Delaunay triangulation and its dual the Voronoi diagram are ubiquitous geometric complexes. From a topological standpoint, the connexion has recently been made between these constructions and the Morse theory of distance functions. In particular, algorithms have been designed to compute the flow complex induced by the distance functions to a point set.

This paper develops the first complete and robust construction of the extended flow complex, which in addition of the stable manifolds of the flow complex, also features the unstable manifolds. A first difficulty comes from the interplay between the degenerate cases of Delaunay and those which are flow specific. A second class of problems comes from cascaded constructions and predicates —as opposed to the standard in-circle and orientation predicates for Delaunay. We deal with both aspects and show how to implement a complete and robust flow operator, from which the extended flow complex is easily computed. We also present experimental results.

Key-words: Voronoï diagrams, Distance functions, Critical points, Morse theory, Morse-Smale diagram, Flow complex.

Construction robuste de flot complexe étendu en dimension trois

Résumé : La triangulation de Delaunay et son dual le diagramme de Voronoi sont des constructions géométriques fondamentales. D'un point de vue topologique, la connexion a été faite récemment entre ces objets et la théorie de Morse des fonctions distance. En particulier, des algorithmes ont été proposés pour calculer le *flot complexe* induit par la fonction distance à un nuage de points.

Ce travail développe le premier algorithme complet et robuste pour le flot complexe étendu, qui outre les variétés stables du flot complexe, contient aussi les variétés instables. Une première classe de difficultés réside dans la gestion des cas dégénérés —ceux spécifiques à Delaunay et ceux spécifiques au flot complexe. Une seconde classe de problèmes vient des prédicats et constructions cascadés —par opposition aux prédicats `in_circle` et `orientation` suffisants pour la construction de Delaunay. Nous indiquons comment gérer ces problèmes, et comment implémenter un opérateur de flot robuste. Celui-ci est alors utilisé pour construire le flot complexe étendu. Des illustrations sont aussi données.

Mots-clés : Diagrammes de Voronoï, Fonctions distances, Points critiques, Theorie de Morse, diagramme de Morse-Smale, Flot Complexe.

1 Introduction

1.1 Morse theory of distance functions

Given a collection of geometric objects, the loci of point equidistant from these objects is a fundamental construction appearing under various names in differential geometry (cut locus, medial axis) [Ber03, BG86], mathematical morphology (medial axis, skeleton) [Ser82], non-smooth analysis (singular set, central set) [Hor94], Computational Geometry (Voronoi diagram), etc. The construction is theoretically fundamental, and has countless practical applications [OC00].

An equally important construction is the collection of level sets of the distance function to these objects. Investigating the evolution of these level sets when the distance increases can be casted into the framework of Morse theory, which is concerned with the study of functions defined on manifolds [Mil63]. In the setting of Computational Geometry (CG) and Geometric Modeling, the framework of Morse theory has been approached from several directions. The development of α-shapes [Ede92] and the investigation of topological properties of collections of (growing) balls [Ede95] was probably the first time notions from differential topology were used in CG —these constructions are essentially concerned with topological events underwent by the level sets of the (power) distance function. In a nearby vein, the precise framework of Morse theory has been applied to distance functions originating in the context of Euclidean Voronoi diagrams for points [Sie99], and a construction termed the *flow complex* was developed in [GJ03] based on properties of the Delaunay and Voronoi diagrams. These veins connected recently since its was shown α-shapes and flow shapes are homotopy equivalent [aJGaMJ03, BG05]. In a somewhat different realm, the distance function to a compact set has been used in mathematical morphology to investigate properties of medial axes and skeletons [Ser82]. Further properties of this function were used in [Lie03] to prove any open bounded subset of $\mathbb{R}^n$ has the same homotopy type than its medial axis. From a global perspective, constructions related to distance functions bridge the gap between local geometric and global topological properties.

Application-wise, distance functions proved recently to convey important informations for the study of Van der Waals models [EFL98], in surface reconstruction [GJ02, Cha03, Ede03, aJGaERaBS05], and shape segmentation [DGG]. Apart from this Euclidean setting, Morse theoretic ideas related to Morse-Smale diagrams have been explored [CCL03] in the realm of Forman's combinatorial Morse theory [For98].

1.2 Extended Flow complex versus Morse-Smale diagram

Following classical terminology in differential topology, a *critical* point of a differentiable function is a point where the gradient of the function vanishes, and the function is called a *Morse* function if its critical points are isolated and non degenerate. Given a Morse function defined over a manifold M, and a critical point p of that function, the stable (unstable) manifold $W^s(p)$ ($W^u(p)$) is the union of all integral curves associated to the gradient of

the function, and respectively ending (originating) at p. The function is termed *Morse-Smale* provided its stable and unstable manifolds intersect transversally [PdM82]. For such a function, the *Morse-Smale complex* is the subdivision of M formed by the connected components of the intersections $W^s(p) \cap W^u(q)$, where p and q range over all critical points.

In the setting of Voronoi diagrams, the focus has been so far on the *flow complex*. In [aJGaMJ03], the construction of stable manifolds of index two saddles has been presented, while a general construction of stable manifolds in any dimension is reported in [BG05].

We define the *Extended Flow Complex* as the collection of stable and unstable manifolds, with the proper incidences. The extended flow complex encloses the flow complex, but is weaker than a Morse-Smale diagram, since intersections between stable and unstable manifolds are not explicitly reported.

1.3 Contributions and paper overview

The algorithms just mentioned operate under genericity hypothesis, and the question of unstable manifolds is not addressed. Most importantly, the fact that robustness issues are not addressed implies these algorithms are bound to fail on general inputs.

In this context, we make the following contributions. First, we precise some points of terminology by (re)defining critical points. Second, we present algorithms for flowing across Voronoi edges and facets, these algorithms being the cornerstone of a complete and robust flow operator. Third, we explain how to use them to construct the extended flow complex. In particular, our presentation provides a unified view of the complex, and avoids the development of dedicated algorithms for stable and unstable manifolds of various indices, as done previously. Degenerate cases and numerical issues are discussed. In particular, we emphasize the fact that contrarily to the construction of the Delaunay triangulation, exact constructions —versus predicates— are mandatory to ensure correctness in the general case.

In section 2, we review basics on the distance function to a compact set, and refine the usual notion of critical point. In section 3, we present the complete road-book to flow across Voronoi faces. Algorithms to flow across Voronoi edges and facets are presented in sections 4 and 5. In section 6, we explain how to construct the extended flow complex. Finally, section 8 presents experimental results.

1.4 Notations

This section is meant as reference for notations. In particular, *undefined notions* are introduced when appropriate in the text. Central to our constructions are the Voronoi and Delaunay diagrams. We shall assume the Voronoi diagram is represented via its dual Delaunay triangulation. Following standard usage, we assume the Delaunay triangulation is given as a collection of simplices with the proper incidences. For example, all Delaunay triangles incident upon an edge e can be accessed by rotating around this edge; two consecutive such triangles define a tetrahedron incident on e. When manipulating Voronoi/Delaunay faces

of all dimensions, we shall use the following Voronoi/Delaunay terminology: Vertex/cell, Edge/facet, Face/edge and Cell/vertex. In particular, an initial out of {V, E, F, C} or {c, f, e, v} identifies unambiguously a Voronoi or Delaunay face. When the dimension is not specified, a Voronoi/Delaunay face are denoted O/O^*. Moreover, the duality operator returning the Delaunay face associated to a Voronoi face, or vice-versa, is denoted with a super-script, e.g. $V^* = c$.

The center of the smallest ball circumscribing a Delaunay simplex of any dimension is denoted z, while the center of the smallest empty ball is denoted y. In particular, recall z always lies on the affine hull of the simplex. Delaunay simplices whose such balls are empty are called Gabriel simplices.

For a set O, its boundary and relative interior are respectively denoted ∂O and $\mathrm{RelInt}(O)$.

Occasionally, to clarify figures, we shall use the signature of a tetrahedron defined as the number of its *critical points* of all dimensions, that is $(4, x, y, z)$ with $4 - x + y - z = 1$.

2 Distance function and critical points

2.1 The distance function d_K to a compact set

Given a compact set K of $\mathbb{R}^d$, the distance function to K is defined by $d_K(p) = \min_{q \in K} d(p, q)$, with $d(p, q)$ the Euclidean distance. Function d_K is not differentiable on the medial axis of K, but it has been shown that a generalized gradient coinciding with $\nabla d_K(p)$ where d_K is differentiable can be defined [Lie03]. To see how, for any point p, consider the set $C(p)$ of contact points to K, i.e. the points realizing the distance $d_K(p)$. Denote $R(p)$ its radius, $d(p)$ the center of the smallest ball containing these contact points, and $r(p)$ the radius of this smallest containing ball. This generalized gradient is defined as [Lie03]:

$$\nabla d_K(p) = \frac{p - d(p)}{R(p)}, \tag{1}$$

and satisfies

$$\nabla d_K(p)^2 = 1 - \frac{r(p)^2}{R(p)^2}. \tag{2}$$

This gradient defines the directions of steepest ascent for the function d_K. It can be shown it defines a *flow*, which tells how a point p moves so as to maximize function d_K.

When the compact set is a collection of sample points, function d_K is easily studied since the medial axis reduces to the $(d-1)$-skeleton of the Voronoi diagram. In particular, if O stands for the relatively open Voronoi face of smallest dimension containing point p, the set $C(p)$ corresponds to the vertices of the simplex O^*. Because point $d(p)$ actually indicates the direction of this generalized gradient, its has been called the *driver* in [GJ03]. Equivalently, the driver is characterized as the point of O^* nearest to p.

2.2 Elements of differential topology

When studying functions on manifolds, and more precisely Morse functions, critical points induce a decomposition of the manifold. More precisely, the manifold has the homotopy type of a CW complex with one cell of dimension k for every critical point of index k. This decomposition is obtained by tracking the topological changes of the level set of the function on the manifold [Mil63]. One change exactly occurs at each critical point, by attaching one cell of dimension k corresponding to the inflow of the critical point.

2.3 Critical points of d_K

The notion of critical point just recalled also applies to the generalized gradient of Eq. (1). However, if one wishes to track topological changes of the level sets of function d_K, the notion of critical point is not sufficient anymore. As illustrated on Fig.1(a,b), the wavefront does not systematically incur a topological change when a point such that $\nabla d_K(p) = 0$ is reached. To account for this subtlety, we define:

Definition. 1 *A point p is called* topologically critical (regular) *if the level set of d_K (does not) incurs a topological change upon crossing point p.*

Following the analysis carried out in [Sie99], we actually have:

Observation. 1 *Point p is* critical *iff it belongs to the* interior *of the convex hull of its contact points $C(p)$.*

Two comments are in order. First, this definition is different from that traditionally used in the context of distance functions to compact sets [Lie03], where a point is termed critical if it belongs to the convex hull of the contact points. Second, in the context of Delaunay - Voronoi, this definition is also different from that using the intersection between the Delaunay and Voronoi faces. In fact, the characterization of critical points from Obs. 1 is more general, since the convex hull of the contact points reduces to a simplex if no degeneracy occurs in Delaunay. Following [Sie99, GJ03], the *index* of a critical point p is $d-k$, with k the dimension of the open Voronoi face of lowest dimension containing p.

Definition 1 can be used to disqualify points with $\nabla d_K(p) = 0$ as critical points, as illustrated on Fig. 2 —refer to section 1.4 for the definition of points y, z. On Fig. 2(a), two such critical points of index 1 and 2 associated to a Delaunay edge and triangle coincide and can be discarded. On Fig. 2(b), two such critical points of index 1 and 2 associated to a Delaunay triangle and tetrahedron can be discarded too. On Fig. 2(c), four such critical points —one of index 1, one of index 3, and two of index 2— can be discarded.

Figure 1: $2d$ examples with $\nabla d_K(p) = 0$ in both cases (a)Point p is topologically regular –the level set does not undergo a topological change when the distance shifts from d_1 to d_2 (b)Point p is topologically critical –a maximum

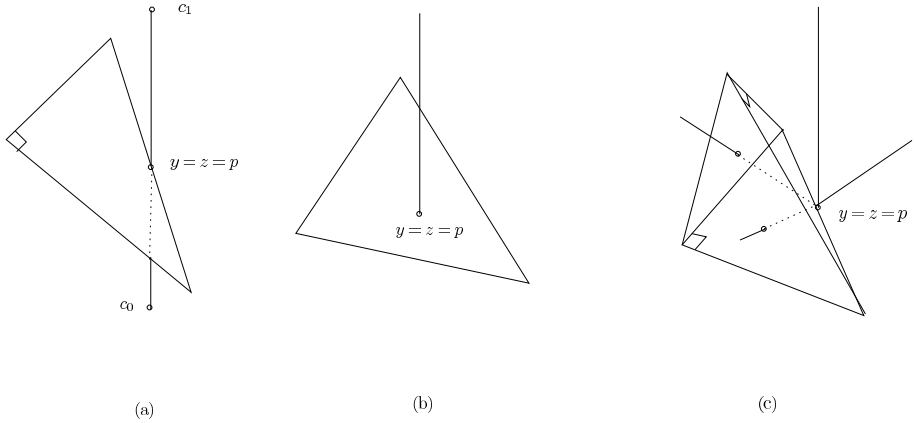

Figure 2: Points p which are topologically regular although $\nabla d_K(p) = 0$ (a)$\partial O^* \cap \text{RelInt}(O) \neq \emptyset$ (b)$\text{RelInt}(O^*) \cap \partial O \neq \emptyset$ (c)Voronoi vertex on an edge. Signature of tetra is $(4, 5, 2, 0)$

3 Flowing across Voronoi objects: the road-book

Describing how one flows faces several types of difficulties: first, one needs to accommodate flow to infinity across unbounded Voronoi faces and across Voronoi rays dual of Delaunay triangles found on the convex hull; second, one needs to take care of flow specific degenerate cases; third, one needs to handle Delaunay specific degenerate cases.

3.1 Flow segment

Since the flow is linear in relatively open Voronoi faces, we shall iteratively follow a trajectory by restricting it to an open Voronoi face. We define:

Definition. 2 *Let p a point we want to flow from. By* combinatorial flow segment*, we refer to the triple: (i) the relatively open Voronoi face S containing the Start point (ii) the relatively open Voronoi face C Crossed from this point (iii) the endpoint Reached on the boundary of S, or infinity if the point flows to infinity. By* flow segment*, we refer to the trajectory followed by point p across the faces of the combinatorial flow segment.*

Practically, a combinatorial flow segment is denoted by a triple $S - C - R$, each letter taken from the symbols {V, E, F, C} to represent a Voronoi face. Given an initial position, flowing consists of computing a sequence of flow segments. Computing a flow segment —the primitive operation, requires identifying the face crossed and finding the trajectory itself from which the face reached is obtained. Flowing across Voronoi edges and faces are described in sections 4 and 5. Before presenting the operations, we discuss the identification of the driver of a given point.

3.2 Drivers

To discuss the possible cases, we distinguish by the dimension of the Voronoi object containing the start-point:
—Starting from the interior of a Voronoi region. The driver is the sample point associated to the Voronoi cell.
—Starting from the relative interior of a Voronoi facet. The driver is the midpoint of the Delaunay edge dual of the facet.
—Starting from the relative interior of a Voronoi edge. The driver is associated to the dual Delaunay triangle or to one of its edges. See Figs. 3, 4, 5 for the possible combinatorial flow segments.
—Starting from a Voronoi vertex. If the Voronoi vertex is critical, it is its own driver. If not, the driver is associated to an edge or a triangle of the Delaunay tetrahedron dual of the Voronoi vertex, see Figs. 6 and 7. A Voronoi vertex driven by a triangle flows along a Voronoi edge. But as illustrated on Fig. 8, the converse is not true, due to a degenerate geometry of the tetrahedron dual of the Voronoi vertex. Consider a Voronoi center c of a non critical tetrahedron driven by the middle d of edge p_0p_1. Let S be the sphere circumscribed to the tetrahedron, S_{01} be the sphere whose diameter is p_0p_1, and B_{01} the ball bounded by S_{01}. Under our hypothesis, the ball B_{01} contains p_2 and p_3. The intersection $S \cap S_{01}$ is a circle C_{01}, and since p_2, p_3 belong to S and are located inside B_{01}, they are located on the lower spherical cap of S bounded by C_{01}. Let p_i stand for p_2 or p_3. If p_i belongs to the interior of this spherical cap, we are in the generic situation of Fig. 7. If p_i belongs to the circle C_{01}, then triangle $p_0p_1p_i$ is rectangle at p_i, and the Voronoi segment $(p_0p_1p_i)^*$ is collinear with the line-segment dc.

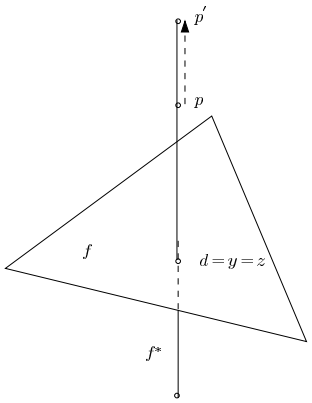

Figure 3: Flow segments E-E-{V,∞}: from a Voronoi edge f^* dual of critical Delaunay triangle f.

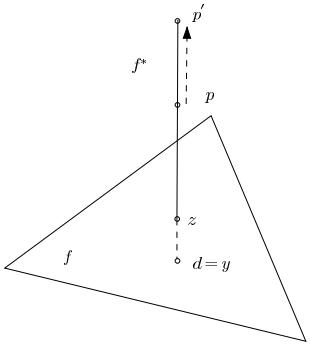

Figure 4: Flow segments E-E-{V,∞}: from a Voronoi edge f^* dual of a non Gabriel (non critical) Delaunay triangle f.

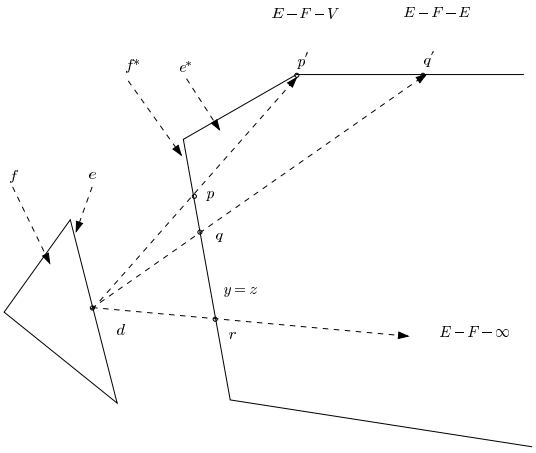

Figure 5: Flow segments E-F-{V,E,∞}: Flow from a Voronoi edge f^* dual of a Gabriel non critical Delaunay triangle f. Driver is associated to edge e

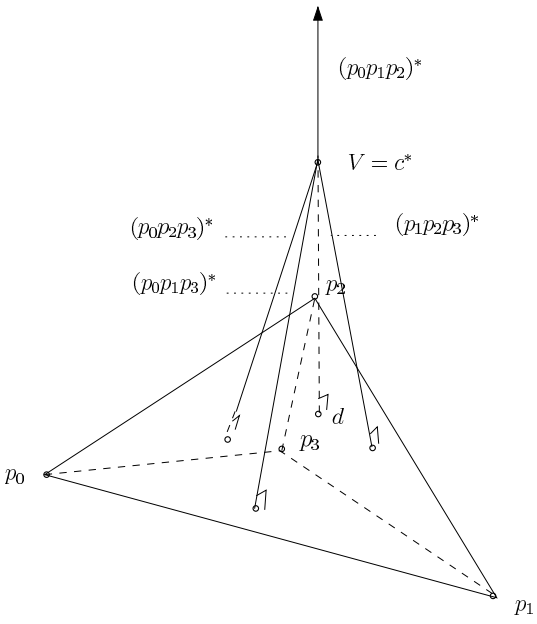

Figure 6: Flow segments V-E-{V,∞}. Signature of the tetrahedron shown is $(4, 6, 3, 0)$.

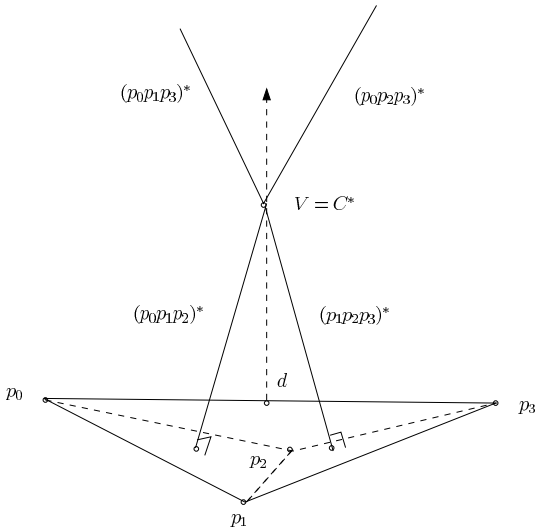

Figure 7: Flow segments V-F-{V,E,∞}. Signature of the tetrahedron shown is $(4, 5, 2, 0)$.

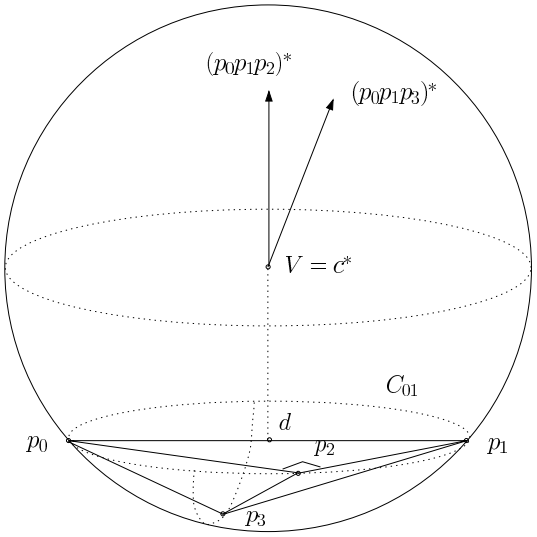

Figure 8: Point p_2 belongs to the minimum-enclosing ball defined by edge p_0p_1: Voronoi edge $(p_0p_1p_2)^*$ is collinear with segment dc

3.3 Enumerating all possible flow segments

Before enumerating all possible flow segments, we need to accommodate the degenerate case in Delaunay corresponding to $n > 4$ co-spherical points. We define:

Definition. 3 *A point p is called a* duplicate *Voronoi vertex if it coincides with at least two circumcenters of tetrahedra featuring co-spherical points. A Voronoi vertex which is non duplicate is called* simple. *A Voronoi edge corresponding to a duplicate Voronoi vertex is called* trivial.

As discussed in section 2, a duplicate Voronoi vertex may be topologically regular. Such a vertex may therefore yield a V-V-V flow segment.

The possible flow segments are listed on Table 1, where S and C respectively refer to the Start and Crossed Voronoi faces. Algorithms for entries marked as [x] are developed in the sequel, while entries marked as [o] are not —they are irrelevant for the calculation of the extended flow complex. Before presenting these algorithms, one can observe that there are actually three types of degeneracies:
—Generic Voronoi face, degenerate flow for selected starting points. This is the E-F-V case depicted on Fig. 5.
—Non generic Voronoi face, non-generic flow. This occurs when flowing from a Voronoi vertex, as on Fig. 8.
—Duplicate Voronoi vertices. This difficulty is independent from the previous two.

$\dim(S)$ | $\dim(C)$	0	1	2	3
0	V-V-V [x]	V-E-{V,∞} [x]	V-F-{V,E,∞} [x]	$\emptyset$
1	$\emptyset$	E-E-{V,∞} [x]	E-F-{V,E,∞} [x]	$\emptyset$
2	$\emptyset$	$\emptyset$	F-F-{V,E,∞} [o]	$\emptyset$
3	$\emptyset$	$\emptyset$	$\emptyset$	C-C-{V,E,F,∞} [o]

Table 1: List of possible flow segments

4 Flowing across a Voronoi edge

We have two cases, depending on whether the start point is a Voronoi vertex or is located in the interior of the edge.

4.1 Cases V-E-{V,∞}

We assume $V = c^*$ is a Voronoi vertex incident to a Voronoi edge $E = f^*$. The flow consists of flowing to the second endpoint of f^*, associated to the tetrahedron neighbor of c across f, or to infinity if f is located on the convex hull. As a degenerate situation, we face the case of a duplicate Voronoi vertex. In that case, moving to the neighbor of c is still correct. After a finite number of such moves, we either end up with a tetrahedron whose Voronoi vertex is a maximum, or we end up on a non-degenerate Voronoi edge and the flow proceeds.

4.2 Cases E-E-{V,∞}

Point p lies in the interior of the edge $E = f^*$ and is driven by a triangle. We have two cases depending on whether E is a Voronoi edge or ray. For a Voronoi edge, we have two sub-cases: if facet f is critical, we flow to the Voronoi vertex located on the same half-Voronoi edge as p; else, we flow to the Voronoi vertex farthest from p. For a Voronoi ray, the strategy follows mutatis mutandis.

5 Flowing across a Voronoi facet

5.1 Overview

Consider a point p on the boundary of a Voronoi face e^*. We assume point p is specified from the smallest dimensional Voronoi object containing it. In particular, if point p coincides with a duplicate Voronoi vertex, we assume it is specified from a Voronoi vertex and not from a trivial Voronoi edge. Given such a point, we wish to find the open Voronoi face crossed —the face itself or one of its boundary edge, together with the point reached by the flow.

Because we need to detect situations such as a flow along a Voronoi edge as on Fig. 8, the algorithm consists of sequentially examining the Voronoi edges and/or rays bounding e^*,

so as to report the Voronoi edge or Voronoi vertex reached. Not surprisingly, the difficulty consists of handling the interplay between flow specific and Delaunay degenerate cases — when the Voronoi vertex V of Fig. 8 is duplicate.

5.2 The generic case

Algorithm. Let p be a point on the boundary of a Voronoi facet $F = e^*$: p is either a Voronoi vertex, or lies in the interior of a Voronoi edge. Let dp^+ be the ray emanating from d and passing through p. Assuming the facet e^* is not Gabriel and since the flow is linear in Voronoi objects, we need to compute the intersection between the ray dp^+ and the boundary of e^*. To see how to proceed, let $e = (p_0p_1)$ the non Gabriel Delaunay edge. To compute the afore-mentioned intersections, we sequentially examine the intersection between the ray dp^+ and the Voronoi edges or rays bounding the facet e^*. Following best practices, we distinguish between predicates and constructions.

Predicates. Consider a Voronoi segment c_ic_{i+1} along the boundary of e^*. To check whether it is intersected by dp^+, since edge e and its dual are orthogonal, it is sufficient to compute the following signs:

$$s_0 = \text{sign}(< dp \wedge dc_i, p_0p_1 >),\ s_1 = \text{sign}(< dp \wedge dc_{i+1}, p_0p_1 >). \tag{3}$$

The predicate for a Voronoi ray is similar. Calling c_i the finite Voronoi vertex and u the unit vector orienting the ray, we compute:

$$s_0 = \text{sign}(< dp \wedge dc_i, p_0p_1 >), \quad \text{and } s_1 = \text{sign}(< dp \wedge u, p_0p_1 >). \tag{4}$$

Definition. 4 *The signature of a Voronoi edge or ray dual of a Delaunay facet f is defined by $\tilde{f} = [s_0, s_1]$, with s_0, s_1 defined by Eqs. (3) or (4).*

The signature of a Voronoi face is defined as the concatenation of the signatures of its Voronoi edges/rays.

The following observations will be helpful in understanding the algorithm below:

Observation. 2 *Let s_i be the sign associated with Voronoi center c_i. One has: $s_i = 0$ iff $p = c_i$, or $p \neq c_i$ and dp is collinear to dc_i.*

Let s_i be the sign associated with the direction u of a Voronoi ray. One has $s_i = 0$ iff dp and u are collinear, and in that case, the sign of the finite Voronoi vertex may be 0 or ± 1.

Construction. The predicates just presented allow the detection of the Voronoi edges intersected at the expense of the evaluation of the sign of a polynomial. Assume we have found a Voronoi edge or ray intersected by the ray dp^+. The construction of p' is easily done by considering the intersection between the Voronoi line-segment or ray with the plane defined by the triple p_1p_2p. This intersection requires manipulating rational numbers.

Notice the construction of point p' needs to be done exactly: on Fig. 9, if point p' lies next to a Voronoi vertex, the rounding errors inherent to floating point computations may yield a constructed point located on the wrong Voronoi edge, or outside the Voronoi edge. In that case, ensuing computation may be erroneous.

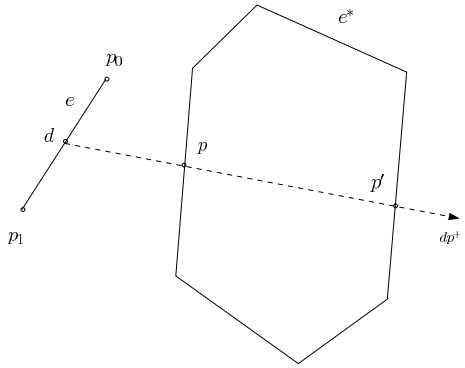

Figure 9: Primitive for flowing across a Voronoi face

5.3 The general case

Exceptional and regular situations. When flowing from a (possibly duplicate) Voronoi vertex across a Voronoi face, since the flow may reach another (possibly duplicate) Voronoi vertex, the signature of the facet contains at most two sequences of the following type, each associated with a (possibly duplicate) Voronoi vertex: $[\pm 1, 0][0, 0]^*[0, \mp 1]$. (The * and $^+$ exponents are used as in regular expression.) For example, the two Voronoi edges incident on a simple Voronoi vertex yield the signature $[\pm 1, 0][0, \mp 1]$, whereas a multiple Voronoi vertex yields the sequence $[\pm 1, 0][0, 0]^+[0, \mp 1]$.

To handle the flow situations listed in Table 1, we first introduce the following exceptional situations: —EX_SEG_VCC: f^* is a trivial Voronoi segment.
—EX_RAY_COLLINEAR: f^* is a ray, dp^+ is collinear with that ray, and p coincides with the finite Voronoi vertex.
—EX_SEG_COLLINEAR: f^* is a non trivial Voronoi segment, dp^+ is collinear with that segment, and p coincides with one of the Voronoi vertices.

Next, we define the following situations, which assume none of the exceptional situations just introduced hold:
—REG_INT_START: The signature of f satisfies $\tilde{f} = [0, \pm 1]$. (If f^* is a ray, notice this subsumes that the first tetrahedron incident on f is finite.)
—REG_INT_END: The signature of f satisfies $\tilde{f} = [\pm 1, 0]$. (If f^* is a ray, notice this subsumes that the first second of f is finite.)
—REG_INT_INTERIOR : dual is a segment or a ray, and the intersection occurs in its interior. That is $\tilde{f} = [1, -1]$ or $\tilde{f} = [-1, 1]$.

Algorithm. To present algorithm `Flow_across_vor_facet`, we shall need the following data structures:
—X: a set containing the Delaunay facets dual of Voronoi edges which are intersected by dp^+, yet are of no interest. If p lies in the interior of a Voronoi edge, X contains the facet dual of that edge; if p is a Voronoi vertex, X contains the two Delaunay facets whose dual Voronoi edges intersect at the Voronoi vertex.
—Y: a list containing Delaunay facets dual of Voronoi edges which are intersected by dp^+ at an endpoint of the Voronoi edge, and which may or may not be valid intersections due to $n > 4$ co-spherical points.
—w: boolean initialized to false stating whether the intersections recorded in Y are valid or not.
—I: a list containing Delaunay facets dual of Voronoi edges defining valid intersections.

Equipped with these data structures, algorithm `Flow_across_vor_facet` sequentially processes the Voronoi edges bounding e^* as indicated in Algorithm 1. Upon termination of the algorithm, one concludes as follows: if $I = \emptyset$, the flow ends at infinity while crossing interior of e^*; if $\mid I \mid = 1$, the flow ends up on a Voronoi edge after to have crossed e^* transversally; if $\mid I \mid = 2$, the flow ends on a Voronoi vertex. If the vertex is duplicate, notice the algorithm records two non trivial Voronoi edges meeting at the vertex.

A final comment is in order. Using the set X to discard selected edges is valid. In a degenerate situation such as that of Fig. 8, or if the flow starts from a point located in the interior of this edge, we may flow along this edge —record in X. But such situations are handled as exceptions and do not resort to X.

Rmk. Due to the convexity of Voronoi facets, the linear scan of Voronoi edges used in Algorithm `Flow_across_vor_facet` can be replaced by a binary search.

6 Computing the extended flow complex

In this section, we show that the construction of stable and unstable manifolds of critical points of indices one and two, which are the difficult cases, easily stems from the algorithms developed in sections 4 and 5. Notice in particular that the construction of unstable manifolds of index one saddles, stable and unstable manifolds of index two saddles resort to the construction of point p' of Fig. 9, and that correctness of the extended flow complex is not ensured in the general case if this construction is not done exactly.

6.1 Stable manifolds of index one saddles

These are just Gabriel edges.

Algorithm 1 Algorithm `Flow_across_vor_facet`

Let e^* be the Voronoi facet
Choose f such that $\tilde{f} \neq [0, *]$
$w \leftarrow false$
for all Delaunay facets f incident on edge e **do**
  Compute signature $\tilde{f}$ of $*^*$
  {Flow to infinity along Voronoi ray}
  if EX_RAY_COLLINEAR **then**
    Flow to infinity; DONE
  {Flow to Voronoi segment endpoint}
  if EX_SEG_COLLINEAR **then**
    Flow to Voronoi vertex; DONE
  {A duplicate Voronoi vertex with $[0,0]$ signature: set boolean}
  if EX_SEG_VCC **then**
    if $0 \in \tilde{f}$AND$f \in X$ **then**
      $w = true$; NEXT
  {Intersection at endpoint and f not forbidden: record in Y}
  if $\tilde{f} = [\pm 1, 0]$ and $f \notin X$ **then**
    record f into Y
  {Closing the block $[\pm 1, 0][0, 0]^*[0, \mp 1]$}
  if $\tilde{f} = [0, \pm 1]$ **then**
    if $f \notin X$ **then**
      record f into Y
    if w **then**
      discard facets in Y
    else
      transfer facets of Y into I
  {Intersection in the interior of the edge}
  if $\tilde{f} = [\pm 1, \mp 1]$ and $f \notin X$ **then**
    record f into I

6.2 Stable manifolds of index two saddles

In [GJ03], a construction of stable manifolds of index two saddles is presented. Its primitive operation consists of flowing across a Voronoi facet e^* so as to find the pre-image by the flow of a point located on a Voronoi edge bounding e^*. Running the algorithm of section 5 backward instead of forward exactly provides this operation.

6.3 Unstable manifolds of index one saddle

Consider an index one critical point associated to a Delaunay edge e. Its outflow reaches the Voronoi edges and vertices bounding the corresponding Voronoi facet. Tracing the flow of Voronoi vertices has been explained above. Consider a Voronoi edge f^* on the boundary of e^*. If it is critical, we are done. If not, the driver of this edge is one of the two edges of its dual triangle, say edge e'. (Notice the third edge of this triangle is edge e.) The image of f^* under the action of the driver defined by e' is a cone in the Voronoi facet e'^*.

Summarizing, computing the unstable manifold of an index one saddle amounts to computing the outflow of (portions of) Voronoi edges and of Voronoi vertices, which is easily done from the algorithms of sections 4 and 5. Finally, one computes their union.

6.4 Unstable manifolds of index two saddles

The unstable manifold of an index two saddle consists of the (open) integral curves traced from the critical point, and either reaching a maximum —possibly at infinity. Each such curve starts with the open line-segment on the Voronoi edge apart from the critical point. Since the flow is linear in Voronoi objects, to trace such a curve, one start from the Voronoi vertex ending the edge. Consider such a vertex. If it corresponds to a maximum —possibly at infinity, we are done. If not, we follow the flow of that vertex. In general, this flow crosses Voronoi facets and edges, and is easily traced from the algorithms of sections 4 and 5.

7 Additional remarks

7.1 Iterated constructions and predicates

In section 5, we have seen how to compute a flow segment across one Voronoi face. In general, computing stable and unstable manifolds requires cascading such constructions, so that the predicates operate on input points and cascaded constructions.

7.2 The Hasse diagram

For selected applications, one is interested in the incidence diagram between the critical points —which we may call the Hasse diagram due to its stratified structure, rather than the geometry of the stable and unstable manifolds. See Fig. 10 for a $2d$ example.

The incidences between the input points and the index one saddles is trivial from the collection of Gabriel edges. So are those between the index two saddles and the maxima from the unstable manifolds of these saddles. To compute the incidences between the index one and two saddles, we either resort to the stable manifolds on index two saddles, of the unstable manifolds of index one saddles.

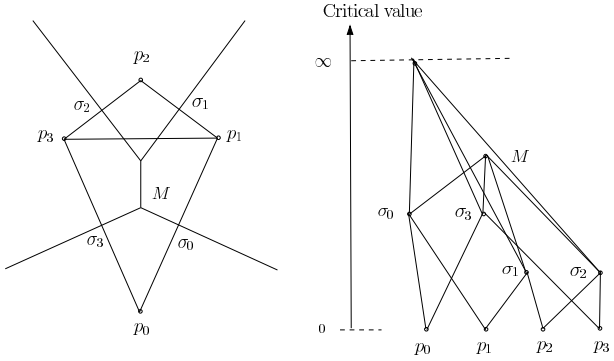

Figure 10: Example Hasse diagram for four points in $2d$

8 Illustrations

The algorithms described have been implemented using the Delaunay triangulation of CGAL, `www.cgal.org`. Due to the criticality of constructions, the kernel used is `CGAL::Exact_predicates_exact_constructions_kernel`. We illustrate the complexity of the flow complex on two models: the vase model (2.7 k points), and a mechanical part (12.5 k points). These two models are real data sets output by scanners. The code was compiled with `gcc version 3.4.4`, and run on a PC at 2GHz.

Table 2 reports statistics on the number of critical points, and on the timings. Columns read as follows: #p: model size in kilo points; idx_k: number of critical points of index k; χ: Euler characteristic; t_D (t_{FC}) time to construct the Delaunay triangulation (the extended flow complex *but* the unstable manifolds of index one saddles). Table 3 provides two sets of statistics. First, the minimum, maximum and average number of triangles in an index two stable manifold —min_t, max_t, μ_t. Second, the same statistics for the number of flow segments along an index two unstable manifold —min_i, max_i, μ_i

As can be seen from Table 2, building the extended flow complex is significantly more demanding than building the Delaunay triangulation. Notice that much faster running times can be achieved for Delaunay using filtered predicates. The same is not possible for the flow complex due to the requirement of exact constructions. Another observation, not present on the table, is that *all* degenerate cases discussed in sections 2.3 —collision and cancellation

of critical points, and section 5 —duplicate Voronoi vertices, actually occur. This owes to the fact that scanned data sets are often rounded on an integer grid.

Table 3 illustrates another main feature of the extended flow complex: the construction is not local, in the sense that stable and unstable manifold may extend arbitrarily far. for example, the minimum number of triangles forming an unstable manifold of index two is three, but this number is as large as two hundreds on our models. The same holds for unstable manifolds. this again stresses the numerical difficulties arising in the course of the construction.

This is illustrated on Fig. 12, which features the critical points of all indices and then largest index two stable manifold. The bottom most line-segment of this manifold, in orange, is a boundary Gabriel edge. The stable manifold extends above in between the two branches of the vase. Color codes for critical points are as follows: index 0 (grey), index 1 (yellow), index 2 (orange), index 3 (red).

	#p	idx_0	idx_1	idx_2	idx_3	χ	t_D	t_{FC}/t_D
vase	2.7k	2714	6126	4341	928	1	2.43	10.3
mec.	12.5k	12593	31632	21886	2846	1	16.1	25.1

Table 2: Critical points and running times

	min_t	max_t	μ_t	min_i	max_i	μ_i
vase	3	264	7.17	1	39	9.14
mec.	3	201	6.40	1	87	15.07

Table 3: Statistics on stable and unstable manifolds of index two saddles

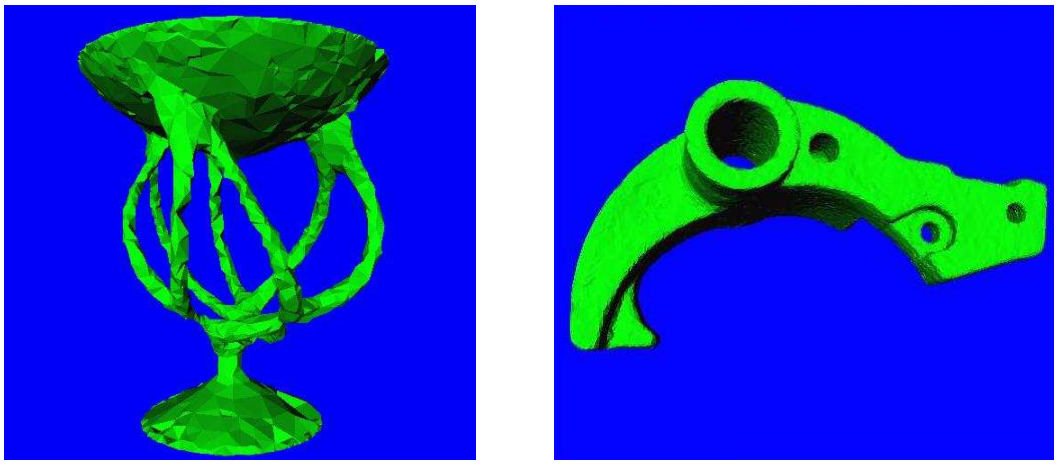

Figure 11: The vase and mechanical models

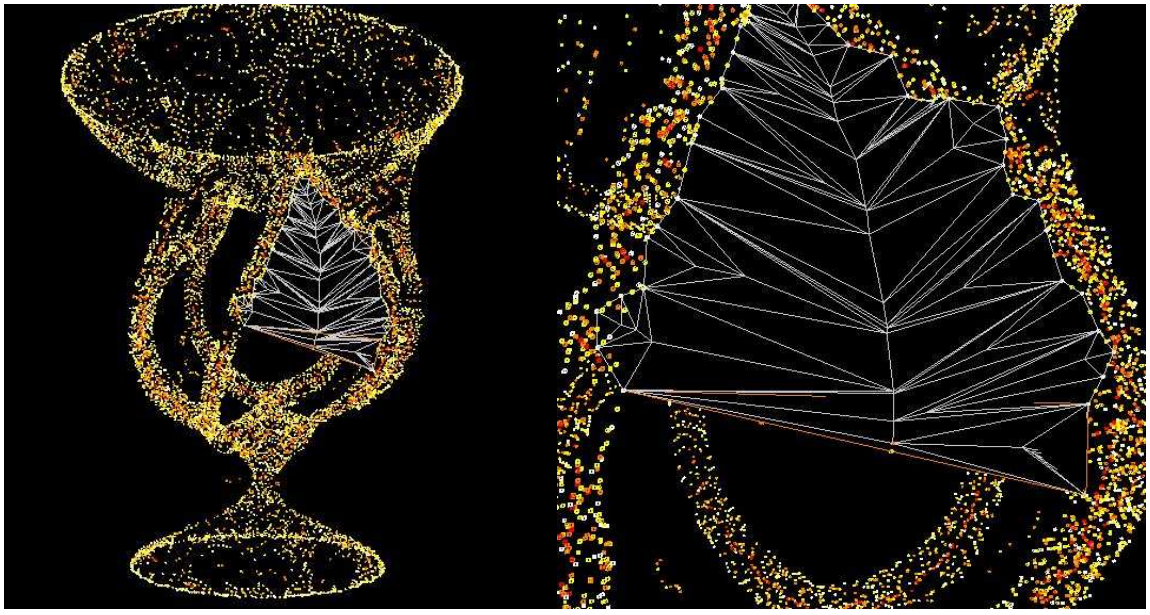

Figure 12: Let: far view of the critical points and of the stable manifold with 264 triangles. Right: closeup.

9 Conclusion

This paper presents the first complete and robust construction of the extended flow complex of the distance function to a collection of points. We show this construction stems directly from the flow operator, i.e. does not require dedicated algorithms for stable and unstable manifolds of various indices. Degenerate cases and numerical issues are discussed. In particular, we emphasize the fact that exact constructions are mandatory to ensure correctness in the general case, a rather annoying constraint yielding cascaded constructions.

Similarly to the Delaunay triangulation a few years ago, which had not had a deep impact due to the lack of robust and efficient algorithms - software, we anticipate this paper will foster the use of flow based constructions in geometric modeling. This paper also open interesting research avenues. First, the cascaded constructions and predicates on these call for the development of arithmetic filters and lazy strategies. Second, investigating whether the intersection of stable and unstable manifolds defines a Morse-Smale diagram is of interest. Third, these stable and unstable manifolds being rather elaborate geometric objects, approximation schemes are also called for.

Acknowledgements. David Cohen-Steiner is acknowledged for discussions.

References

[aJGaERaBS05] T.K. Dey , J. Giesen , E. Ramos , B. Sadri. Critical points of the distance to an epsilon-sampling on a surface and flow based surface reconstruction. In *ACM SoCG*, 2005.

[aJGaMJ03] T. Dey , J. Giesen , M. John. Alpha-shapes and flow shapes are homotopy equivalent. In *35th Annual ACM Symposium on Theory of Computing (STOC)*, 2003.

[Ber03] M. Berger. *A Panoramic View of Riemannian Geometry*. Springer, 2003.

[BG86] J. Bruce and P. Giblin. Growth, motion and 1-parameter families of symmetry sets. *Proc. R. Soc. Edinb., Sect. A*, 104:163–186, 1986.

[BG05] K. Buchin and J. Giesen. Flow complex: General structure and algorithm. In *CCCG*, 2005.

[CCL03] F. Cazals, F. Chazal, and T. Lewiner. Molecular shape analysis based upon the morse-smale complex and the connolly function. In *ACM Symposium on Computational Geometry*, 2003.

[Cha03] R. Chaine. A convection geometric-based approach to surface reconstruction. In *Symp. Geometry Processing*, pages 218–229, 2003.

[DGG] T. K. Dey, J. Giesen, and S. Goswami. Shape segmentation and matching with flow discretization. In F. Dehne, J.-R. Sack, and M. Smid, editors, *Workshop Algorithms Data Strucutres*, pages 25–36.

[Ede92] H. Edelsbrunner. Weighted alpha shapes. Technical Report UIUCDCS-R-92-1760, Dept. Comput. Sci., Univ. Illinois, Urbana, IL, 1992.

[Ede95] H. Edelsbrunner. The union of balls and its dual shape. *Discrete Comput. Geom.*, 13:415–440, 1995.

[Ede03] H. Edelsbrunner. Surface reconstruction by wrapping finite point sets in space. In B. Aronov, S. Basu, J. Pach, and M. Sharir, editors, *Ricky Pollack and Eli Goodman Festschrift*, pages 379–404. Springer-Verlag, 2003.

[EFL98] H. Edelsbrunner, M. Facello, and J. Liang. On the definition and the construction of pockets in macromolecules. *Discrete Appl. Math.*, 88:83–102, 1998.

[For98] R. Forman. Morse theory for cell complexes. *Advances in Mathematics*, 134:90–145, 1998.

[GJ02] J. Giesen and M. John. Surface reconstruction based on a dynamical system. In *Proceedings of the 23rd Annual Conference of the European Association for Computer Graphics (Eurographics), Computer Graphics Forum 21*, pages 363–371, 2002.

[GJ03] J. Giesen and M. John. The flow complex: A data structure for geometric modeling. In *ACM SODA*, 2003.

[Hor94] L. Hormander. *Notions of convexity*. Birkhauser, 1994.

[Lie03] A. Lieutier. Any open bounded subset of $\mathbb{R}^n$ has the same homotopy type than its medial axis. In *ACM Solid Modeling*, 2003.

[Mil63] John W. Milnor. *Morse Theory*. Princeton University Press, Princeton, NJ, 1963.

[OC00] A. Okabe and B. Boots K. Sugihara S. Nok Chiu. *Spatial Tessellations: Concepts and Applications of Voronoi Diagrams (2nd Ed.)*. Wiley, 2000.

[PdM82] J. Palis and W. de Melo. *Geometric Theory of Dynamical Systems*. Springer, 1982.

[Ser82] J. Serra. *Image Analysis and Mathematical Morphology*. Academic Press, London, UK, 1982.

[Sie99] D. Siersma. Voronoi diagrams and morse theory of the distance function. In O.E. Barndorff-Nielsen and E.B.V. Jensen, editors, *Geometry in Present Day Science*. World Scientific, 1999.

Contents

Unité de recherche INRIA Sophia Antipolis
2004, route des Lucioles - BP 93 - 06902 Sophia Antipolis Cedex (France)

Unité de recherche INRIA Futurs : Parc Club Orsay Université - ZAC des Vignes
4, rue Jacques Monod - 91893 ORSAY Cedex (France)
Unité de recherche INRIA Lorraine : LORIA, Technopôle de Nancy-Brabois - Campus scientifique
615, rue du Jardin Botanique - BP 101 - 54602 Villers-lès-Nancy Cedex (France)
Unité de recherche INRIA Rennes : IRISA, Campus universitaire de Beaulieu - 35042 Rennes Cedex (France)
Unité de recherche INRIA Rhône-Alpes : 655, avenue de l'Europe - 38334 Montbonnot Saint-Ismier (France)
Unité de recherche INRIA Rocquencourt : Domaine de Voluceau - Rocquencourt - BP 105 - 78153 Le Chesnay Cedex (France)

Éditeur
INRIA - Domaine de Voluceau - Rocquencourt, BP 105 - 78153 Le Chesnay Cedex (France)
http://www.inria.fr
ISSN 0249-6399